

Achieving Time Domain Transmission Sensing with Fully Passive UHF RFID Tags

Newton Fonsêca^{*(1)}, Ahmed Rennane⁽²⁾, Raimundo Freire⁽¹⁾, Smail Tedjini⁽²⁾ and Glauco Fontgalland⁽¹⁾

(1) Federal University of Campina Grande, Campina Grande, Brazil

(2) Université Grenoble Alpes, Grenoble INP, Valence, France

Abstract

In this paper, it is discussed the simulation and realization of a complete RFID UHF passive Time Domain Transmission sensor tag. A low power sensor interface circuit is described and integrated with a passive tag. Any standard RFID UHF reader can access the sensor data by reading the tag memory. The sensor was tested under saline water solutions, where 10 distinct dielectric constants were evaluated. It was found a 5.72 RMSE from the measurements obtained by dielectric probe and VNA set-up, operating at 301 MHz.

1 Introduction

Over the last decade, Time Domain Transmissometry (TDT) has been a growing technique to access medium permittivity measurements. Similarly to traditional Time Domain Reflectometry (TDR), TDT sensors makes use of the signal propagation delay between the input and output ports of a transmission line probe sensor inserted in a material under test (MUT). In TDT, the first detected pulse at the end of the line is the measuring signal, thus, multiples reflections due to the material and line inhomogeneities does not affect the signal interpretation, as reported in [1].

TDT technique has been achieving satisfactory performance in applications as soil moisture [2] and liquid flow[3] sensing. Related reports has shown soil moisture TDT based sensors with comparable performances to TDR complex set-ups, however, with a tenth of the price [4].

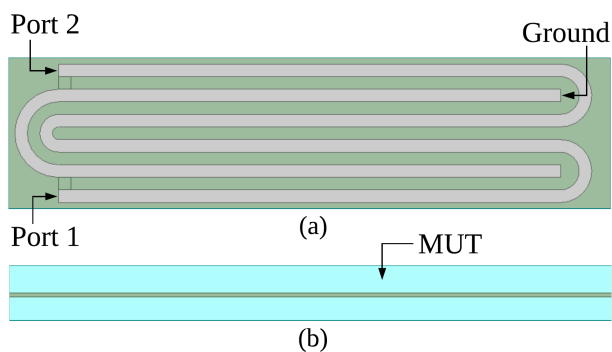


Figure 1. (a) Sensor top view. (b) Sensor side view.

In this paper, it is discussed the simulation and realization

of a complete RFID UHF passive TDT sensor tag. We demonstrate the viability to integrate a low power interface circuit to exploit the sensor propagation delay proprieties in order to access the medium permittivity. The sensor was tested under saline water solutions, where 10 different dielectric constants were evaluated. It was found a 5.72 RMSE (Root Mean Square Error) from the measurements obtained by a Keysight N9912A FieldFox and Agilent 85070E Dielectric Probe Kit, operating at 301 MHz.

2 System Description

2.1 TDT Sensor Development

The developed sensor is based on the measurement of the signal propagation velocity in a given medium, that is

$$c = \frac{c_0}{\sqrt{\epsilon_r \cdot \mu_r}} \quad (1)$$

where ϵ_r and μ_r are the medium relative dielectric permittivity and magnetic permeability, respectively, and c_0 is the speed of light in vacuum. In case of non-magnetic materials medium, μ_r is 1, therefore, ϵ_r determines the signal propagation velocity. Based on this principle, it was designed and simulated on ANSYS HFSS the sensor probe shown in Fig. 1.

The designed sensor was realized under a single layer, 1.6 mm thick FR4 substrate, with 36 μm copper thickness. In order to impose a significative delay between the signals presented on ports 1 and 2, the signal travelling path was designed 87.8 cm long, 5 mm wide, with a gap of 5 mm between each conductor. The medium conductivity influences on the travelling signal attenuation, hence, to avoid this effect, it was also included in the simulation a 35 μm thick acrylic coating layer for all probe conductors. In fact, this coating layer reduces the sensor sensitivity, however, this trade-off reduces considerably the signal conditioning circuit complexity, and consequently, the power consumption.

In order to verify the sensor signal propagation velocity behavior when exposed to a MUT, it was included in the simulation an additional 5 mm plane layer on both sensor sides. We performed simulations from 1 MHz to 1 GHz and exported the S-Parameters into an equivalent discrete model

block. This procedure were performed by setting MUT to air and distilled water. Finally, in a discrete circuit level, the imported S-Parameters model block was excited by a step voltage source, with amplitude of 3.3 V, 50Ω series resistance, and 1 ns rising time. It was observed a 12 ns time delay difference between the simulations performed in air and distilled water, as shown in Fig. 2.

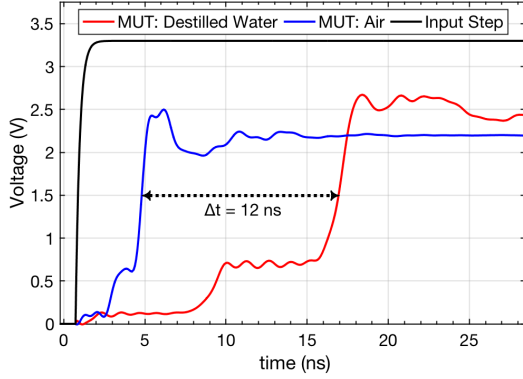


Figure 2. Sensor step responses in contact with distilled water and air.

2.2 UHF RFID Tag Integration

The complete proposed system, shown in Fig. 3, is composed by the integration of the smart tag SL900A (AMS AG) and the low power microcontroller (MCU) PIC16LF1707 (Microchip Inc.). This MCU consumes $32\ \mu\text{W}/\text{MHz}$. Since the SL900A features a SPI bus that allows an external device to perform read and write operations on a 1152 bytes memory bank, it is a convenient method to exchange data between the developed sensor and any standard RFID UHF reader. Furthermore, the SL900A includes a RF rectified power output, V_{pos} , that is capable to supply a maximum $680\ \mu\text{W}$ external load. This power is used to supply the MCU, which operates at 16 MHz and consumes $512\ \mu\text{W}$.

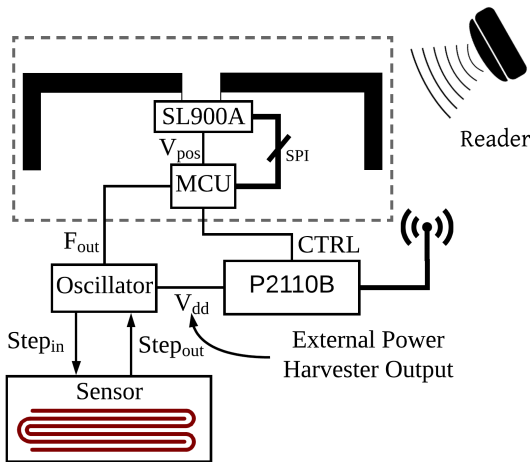


Figure 3. Complete system block diagram.

To supply the interface sensor circuit, it was used an external RF power harvester, based on P2110B (Powercast Co.).

This device implements a complete RF to DC converter, that can be controlled by a MCU. The harvested power is stored on a 50 mF capacitor and its integrated boost converter outputs stable 3.3 V on V_{dd} .

The MCU coordinates the entire sensor reading operation. When the RFID reader is interrogating the tag, V_{pos} outputs power to supply the MCU. After waking up, the MCU detects when there is enough accumulated power available on P2110B storage capacitor to ensure a proper sensor interface circuit operating time and, by setting CTRL, switches on the V_{dd} . Once the interface sensor circuit starts to operate, the MCU reads the output sensor frequency. This data is stored in 4 addressable bytes on the SL900A memory.

3 Experimental Verification

3.1 System Validation

In TDT sensing, the operating bandwidth is directly associated to the excitation rise time step. For the developed sensor interface oscillator, which produces a 1 ns rise time step, the majority signal energy spectra will be concentrated in the frequency around 350 MHz [5].

When the sensing MUT is air, the measured $f_{out=air}$ frequency was 8.9 MHz. This represents a 12.3 ns period delay shift from the reference oscillator, without the delay produced by the sensor, which operates at 10 MHz. For another materials with greater dielectric constants, $f_{out=MUT}$ is expected to decrease, due to the lower sensor signal propagation velocity. By referring to (1), one can calculate the period $T_{out=MUT}$ by an incremental time delay according to

$$T_{out=MUT} = T_{out=air} + \frac{2 \cdot L \cdot (\sqrt{\epsilon_{MUT}} - 1)}{c_0} \quad (2)$$

where L is the sensor transmission line length.

In order to read the SL900A memory, it was used the IM-PINJ Speedway R420 RFID UHF reader. The transmission power was set to 2 W ERP, operating at 868 MHz. From the first reader interrogation, it was observed a 5 seconds delay for detecting updated sensor data the on the SL900A memory. This delay comprises the required P2110B storage capacitor charging time. The test was performed with the reader positioned 1.5 meters away from the tag.

3.2 Water Measurements

Distilled water dielectric constant, at 25 °C, is approximately 80. However, for a given frequency, the increment of salt concentration increases the dielectric loss whereas decreases the dielectric constant [6]. In order to investigate the actual operating sensor frequency, it were performed measurements with water under different NaCl concentrations. In addition to the developed sensor, the measurements were also performed, for each sample, with an Agilent 85070E Dielectric Probe Kit and a Keysight N9912A FieldFox, as shown in Fig. 4.

